Vermeulen *et al. J Wireless Com Network* (2021) 2021:87
https://doi.org/10.1186/s13638-021-01940-4

EURASIP Journal on Wireless Communications and Networking

RESEARCH Open Access

Performance analysis of in-band collision detection for dense wireless networks

Tom Vermeulen[1], Brecht Reynders[1], Fernando E. Rosas[2,3,4], Marian Verhelst[1] and Sofie Pollin[1*]

*Correspondence:
sofie.pollin@kuleuven.be
[1] ESAT-WAVECORE, KU Leuven, Kasteelpark Arenberg 10, 3001 Heverlee, Belgium
Full list of author information is available at the end of the article

Abstract

With the massive growth of wireless networks comes a bigger impact of collisions and interference, which has a negative effect on throughput and energy efficiency. To deal with this problem, we propose an in-band wireless collision and interference detection scheme based on full-duplex technology. To study its performance, we compare its throughput and energy efficiency with the performance of traditional half-duplex and symmetric in-band full-duplex transmissions. Our analysis considers a realistic protocol and overhead modeling, and a measurement-based self-interference model. Our results indicate that our proposed collision detection scheme can provide significant gains in terms of throughput and energy efficiency in large wireless networks. Moreover, when compared to half-duplex and symmetric full-duplex, our analysis shows that this scheme allows up to 45% more nodes in the network for the same energy consumption per bit. These results suggest that this could be an enabling technology towards efficient, dense wireless networks.

Keywords: In-band full-duplex, Collision detection, Software-defined radio

1 Introduction

Network densification has been identified as one of the major challenges for future communication systems, as the continuously increasing number of wireless mobile devices generates unprecedented coexistence problems [1]. The ongoing densification in space and frequency forces devices to compete for increasingly scarce communication resources [2], raising the amount of interference and the frequency of transmission collisions. Moreover, interference and collisions are specially difficult to control because of the hidden terminal problem, which is a consequence of the limited sensing ability of wireless devices [3]. Collisions and interference, aggregated by the hidden terminal problem, are fundamental performance bottlenecks for dense wireless networks [4, 5].

Collisions, coming from nodes using the same Medium Access Control (MAC) protocol, and interference, coming from nodes outside the network, waste valuable transmission time and radiated power, having a negative impact on the energy efficiency, throughput and delay of the system. Moreover, existing MAC protocols rapidly become inefficient in dense wireless networks. For example, the collision avoidance mechanism of the well-known Carrier Sense Multiple Access (CSMA)

Springer Open

© The Author(s) 2021. **Open Access** This article is licensed under a Creative Commons Attribution 4.0 International License, which permits use, sharing, adaptation, distribution and reproduction in any medium or format, as long as you give appropriate credit to the original author(s) and the source, provide a link to the Creative Commons licence, and indicate if changes were made. The images or other third party material in this article are included in the article's Creative Commons licence, unless indicated otherwise in a credit line to the material. If material is not included in the article's Creative Commons licence and your intended use is not permitted by statutory regulation or exceeds the permitted use, you will need to obtain permission directly from the copyright holder. To view a copy of this licence, visit http://creativecommons.org/licenses/by/4.0/.

technique is only efficient for a small number of nodes, hence the densification of CSMA networks decreases the total network throughput and increases the delay [6]. In addition, it has been shown that the energy consumption of networks based on CSMA increases exponentially with respect to the number of nodes and the total network throughput [7]. The main problem is that—unlike in wired systems—wireless nodes under this scheme are unable to detect collisions in real-time and abort their transmission. Moreover, the lack of instantaneous collision feedback makes them waste the scarce wireless medium with transmissions that are not going to be decoded anyway.

1.1 Related work

Several state-of-the-art techniques have been proposed to improve the performance of CSMA networks by detecting collisions early. In [8], a collision notification scheme is presented, where the receiving node detects collisions and transmits a unique signature to notify the transmitter, who is constantly looking for this signature. Although this scheme provides some throughput improvements by detecting collisions due to the shortened collision time, it does not solve the hidden terminal problem. In [9], a wireless CSMA Collision Detection (CSMA/CD) scheme is presented, the collisions are detected by randomly switching off the transmitter during transmission and listening for collisions. The authors show improvements in throughput, but this constant switching between transmit and receive state introduces a significant overhead. Another MAC protocol, presented in [10], uses pulses in an out-of-band control channel for collision detection and a clear to send signal to avoid hidden terminals. The protocol uses extra bandwidth and requires two transceivers on different frequencies. Moreover, the protocol is not able to detect interference from other networks if they do not follow the same protocol. In [11] another collision detection scheme for WiFi is analyzed, showing that it can increase the throughput. They conclude that collision detection can increase the throughput if the MAC parameters are chosen correctly. However, they do not analyze the performance for dense networks and only look at the throughput of their scheme, hence neglecting the full system energy consumption.

Ideally, collisions should be detected as soon as possible in order to abort the transmission, saving energy and bandwidth. Detecting collisions while transmitting poses a number of important technical challenges, as for this task the transmitted signal is experienced as Self-Interference (SI), which may be many orders of magnitude larger than the colliding signal that arrives after being attenuated by path loss [12]. This problem is similar to the one found in In-Band Full-Duplex (IBFD), where devices transmit and receive data at the same time and on the same frequency. Key ingredients for making IBFD work are efficient methods of Self-Interference Cancellation (SIC), which usually combine various analog and digital techniques. If the SI signal is canceled below the noise floor, IBFD can potentially double the physical layer throughput without increasing the bit error rate and the frequency usage [13]. Recently, the practical feasibility of IBFD transceivers that efficiently cancel the SI has been demonstrated in a number of testbeds [13, 14].

1.2 Problem statement

From the previous discussion, it is natural to ask if IBFD technology could be used to design a MAC protocol for dense wireless networks. Our main idea, which is explored in this paper, is to use SIC not to increase the bidirectional throughput, but to implement a mechanism of real-time collision detection and notification. In this way, the receiver can sense collisions during reception as soon as they take place, and provide real-time feedback to the transmitter over the full-duplex link if the incoming frame has to be aborted. This provides two direct benefits: save energy at both colliding nodes and free up the wireless spectrum for other users, i.e., increase throughput.

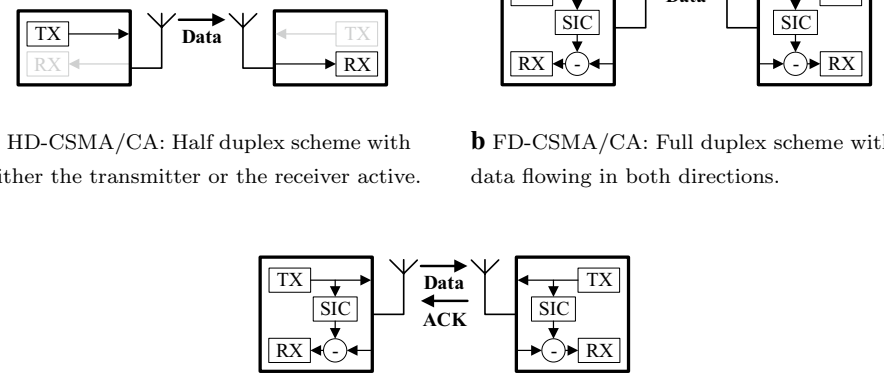
Our previous work [15–17] has shown some of the promising benefits that such a protocol might introduce for wireless sensor networks in order to avoid the collision and interference waste. A slotted version of the protocol was discussed in [15], where it was shown how an IBFD-based collision detection scheme can improve the energy efficiency and reduce the delay of networks in saturated and unsaturated conditions when compared to half-duplex networks. This work was extended in [17], where an unslotted version of the protocol was presented and analyzed. Finally, [16] showed how the energy efficiency can be further improved by introducing a scalable SIC module, which dynamically enables or disables different cancellation stages.

1.3 Contributions

To complement our previous work, the main goal of this paper is to analyze not only the energy efficiency but also throughput of our wireless in-band collision detection scheme and compare it with traditional full-duplex bidirectional transmissions. We also aim to compare these two schemes with Half-Duplex CSMA Collision Avoidance (HD-CSMA/CA) transmissions, in order to generalize the ideas discussed in [15–17] within a single novel theoretical framework. Moreover, our previous work was based on numerical evaluations of [18], while the results of this framework have been verified with novel ns-3 simulations and measurements. This allows us to compare these schemes not only in saturated traffic but also in unsaturated traffic. Our results show that our in-band collision detection scheme outperforms the other two schemes in terms of energy efficiency for high throughput networks and when the number of users in the network is high. Looking at throughput, we see that traditional full-duplex transmissions are only beneficial in symmetric saturated traffic conditions. In all other scenarios, our proposed collision detection scheme has similar throughput. Please note that full-duplex schemes, in which both the transmitter and receiver are active during a transmission, are not impacted by the hidden node problem. This is because any contending node that can cause interference will necessarily hear the receiver's signal. The hidden node problem is, hence, not considered in this paper, as it would not affect the performance of the full-duplex schemes.

1.4 Methodology

In this work, we start with a mathematical model for the energy and the performance for three different MAC schemes: HD-CSMA/CA, Full-Duplex CSMA Collision Avoidance (FD-CSMA/CA) and In-Band CSMA Collision Detection (IB-CSMA/CD).



a HD-CSMA/CA: Half duplex scheme with either the transmitter or the receiver active.

b FD-CSMA/CA: Full duplex scheme with data flowing in both directions.

c IB-CSMA/CD: Collision detection scheme where data is send in one direction and collision information in the other.

Fig. 1 Comparison of the three schemes considered in this paper

These closed-form models depend on a set of variables that depend on the scenario and traffic load and can be determined analytically for ideal scenarios, such as saturated conditions. The model allows for a protocol comparison for those ideal scenarios. In a second step, we simulate more practical scenarios in ns-3, and show that the proposed MAC layer is able to obtain important improvements in all scenarios. As more collisions occur during saturated conditions, our simulations indeed confirm that the performance gains in non-saturated simulated scenarios are lower but still relevant. In our paper, we do a performance and energy analysis, both using ideal analytical and more realistic ns-3 simulations, as explained below.

1.5 Organization of this paper

This paper is organized as follows, Sect. 2 presents an overview of the MAC schemes considered in this paper. In Sect. 3 our performance model is presented, followed by some simulation results in Sect. 4. Next, in Sect. 5, we formulate a mathematical model that describes the energy consumption of the three schemes under diverse traffic conditions, and symmetric or asymmetric uplink versus downlink data flow, followed by an analysis of the energy efficiency in Sect. 6. Finally, in Sect. 7, we draw some conclusions.

2 Overview of MAC schemes

In this paper, we do an energy and throughput comparison of half-duplex transmissions, symmetric in-band full-duplex transmissions and transmissions with in-band collision detection. Figure 1 introduces all three schemes considered in this paper. In the sequel, Sect. 2.1 provides an overview of the legacy HD-CSMA/CA protocol, followed by the full-duplex version of the same protocol in Sect. 2.2. Section 2.3 introduces our proposed IB-CSMA/CD.

2.1 HD-CSMA/CA

In contention-based systems like WiFi [19] and ZigBee [20] the most commonly used medium access control scheme is CSMA, which in this paper is denoted as HD-CSMA/CA (Fig. 1a). A half-duplex transceiver activates either its transmitter or receiver and only one node can be transmitting at a given time. This scheme uses carrier sensing to ensure that the wireless medium is unoccupied before transmitting a packet. If the wireless medium is occupied, the device performs a *random backoff* by adding a random delay to the transmission to avoid colliding with the transmission that is taking place. The backoff time increases exponentially with each backoff to further avoid collisions. A collision occurs when either the carrier sensing mechanism fails due to hidden terminals or when two or more nodes sense the channel unoccupied. Hence, the hidden node problem only affects this half-duplex scheme. As our analyses do not include hidden nodes, the performance results for the HD-CSMA/CA scheme ought to be considered optimistic upper bounds.

2.2 FD-CSMA/CA

CSMA Collision Avoidance (CSMA/CA) can also be implemented over full-duplex transmissions, which is denoted as FD-CSMA/CA (Fig. 1b). Here SIC is used to remove all or part of the self-interference from the received signal. This creates a self-interference free downlink channel, which can be used to transmit data in both directions [21]. Besides its transmitter chain, a full-duplex transceiver needs to activate its receiver chain and self-interference cancellation. If both nodes in a link have data to send to each other the receiver will also become a transmitter, potentially doubling the link throughput. If only one of the participating nodes has data to send, this scheme reduces to the regular HD-CSMA/CA case.

Interestingly, this scheme is able to mitigate the hidden terminal problem when there is a full-duplex transmission, as the signal radiated by the receiver creates a busy signal to its neighboring nodes. Unfortunately, this only works either when the receiver has data to send or in asymmetric scenarios where the performance is affected by the hidden node problem in a similar way as the half-duplex schemes. Besides mitigating the hidden terminal problem, FD-CSMA/CA also improves access point (AP) fairness, as it gives the AP a downlink slot every time a node acquired the medium [21]. Unfortunately, it does not reduce the collision time and therefore still wastes resources during collisions and interference, because collisions are still fully transmitted.

2.3 IB-CSMA/CD

Our proposed scheme uses CSMA with in-band collision detection, which is denoted as IB-CSMA/CD. The setup uses self-interference cancellation to clean up the received signal, as described in Sect. 2.2. In this setup the uplink is used to transmit sensor data to the central node, while the downlink can be used as an instantaneous control channel (Fig. 1c). Therefore, data is transfered following a half-duplex protocol, but simultaneously during the transmission collisions are detected and instantaneous feedback information is provided. This can be considered as an in-band full-duplex system where data

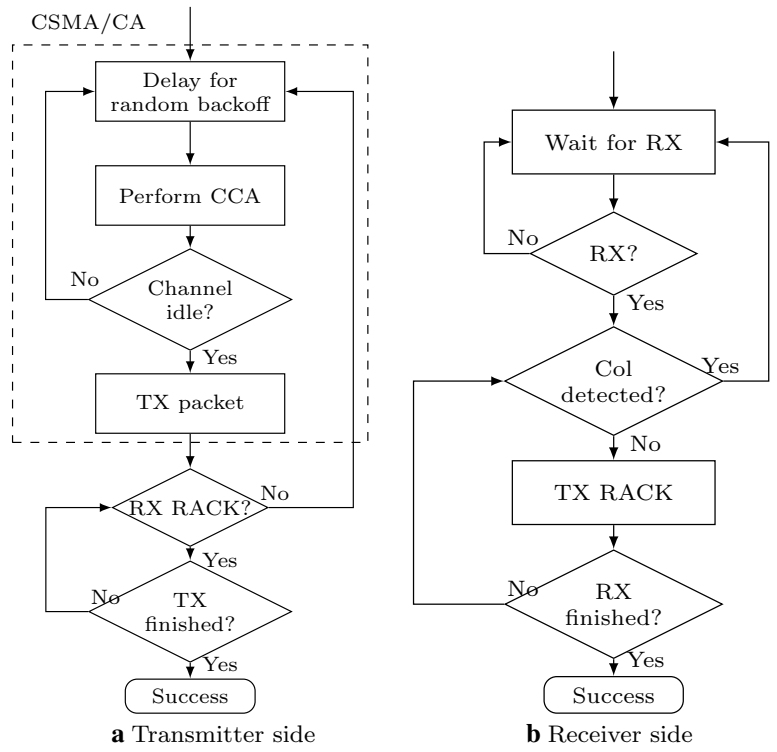


Fig. 2 Flowchart of the IB-CSMA/CD algorithm

is transmitted in the uplink and collisions or interference are simultaneously detected in the downlink. Our earlier work [15, 17] proposed the IB-CSMA/CD scheme to leverage this information to optimize throughput, delay and energy.

Our IB-CSMA/CD protocol is described in Fig. 2. At the transmitter side (Fig. 2a), the node follows the standard HD-CSMA/CA protocol to transmit the packet. At the receiver side (Fig. 2b), the node starts its collision detection, upon receiving the beginning of the payload. If it does not detect any collision it starts transmitting a Real-time Acknowledgment (RACK) on the downlink slot. This is then received by the transmitting node who keeps on transmitting as long as it receives the acknowledgment. In this paper, we assume it is possible for the receiving node to detect collisions during the reception of the packet, which can be done using physical layer information, like the confidence levels from SoftPHY [22] for example.

Our algorithm on a timescale is presented in Fig. 3. Without a collision (Fig. 3a), the receiver immediately starts transmitting the RACK after decoding the header and the transmission continues. When a collision happens (Fig. 3b), either the packet will not be detected or the receiver will detect both the packet and the collision. In both cases, the receiver will not transmit the RACK and the transmitter will stop its transmission. Similarly, when interference is present (Fig. 3c), the receiver will detect this and stop its RACK transmission. The transmitter will react to this by aborting its transmission. The previous discussion clearly shows the difference with other schemes like CSMA Collision Notification (CSMA/CN) [8]. In this case of CSMA/CN, the notification is only transmitted when a collision is detected. However this poses two problems: First, if there

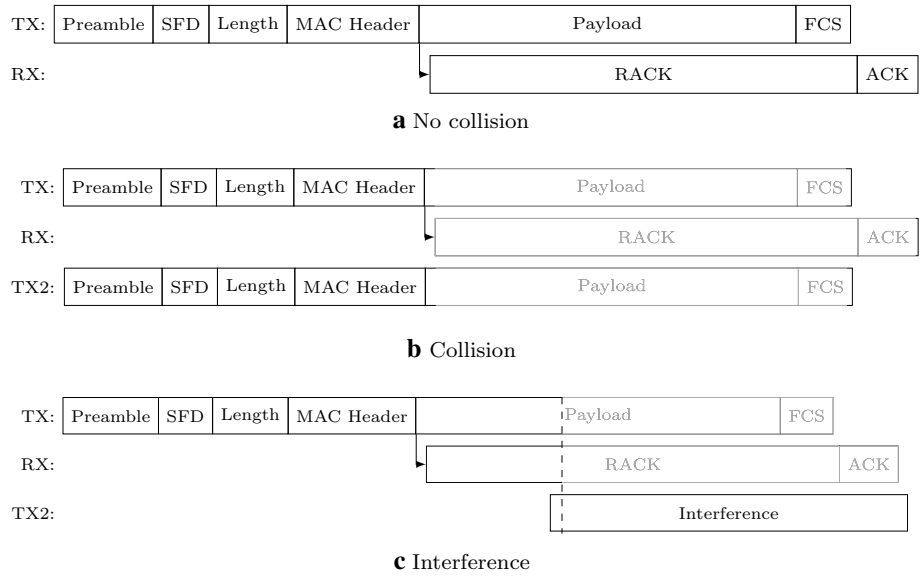


Fig. 3 Different time frames of the IB-CSMA/CD algorithm

is a collision on the header, the packet will not be correctly detected and no notification will be transmitted; Second, if there is a collision on the notification, the transmitter will not be able to detect this. Our scheme does not have these problems as in both situations the transmitter will abort its transmission.

The instantaneous acknowledgment not only enables collision detection at the transmitter side but also mitigates the hidden terminal problem in all scenarios, because the receiver is continuously transmitting feedback information. These feedback packets are sensed by the surrounding nodes and makes them defer their transmission. If the network consists of a combination of IBFD and legacy, half-duplex, nodes, then these half-duplex nodes will also find the channel occupied by the instantaneous acknowledgment, therefore the hidden terminal problem is also solved for these nodes.

It is clear that if one can decrease the collision time, one increases the overall throughput of the system. This will be shown in the next section. However, to achieve this there is an added energy cost for the instantaneous acknowledgment compared to half-duplex. These trade-offs will be investigated in Sect. 5.

In the performance analysis, we will further focus on comparing the efficiency of the three schemes in fair and realistic traffic scenarios. We will focus on scenarios where the number of retransmissions is exactly the same for each protocol, which means that we do not consider the hidden node problem.[1] These conditions provide a fair and easy to understand setup, over which differences in energy and protocol overheads of each scheme best can be best understood.

[1] When hidden nodes will be added, the half-duplex scheme will suffer in all traffic conditions, and the full-duplex scheme will suffer in very asymmetric traffic conditions. The proposed IB-CSMA is insensitive to the hidden node problem. See Sect. 2.1.

3 Performance model

In this section, we develop a model for the assessment of the performance of the three types of wireless links studied in Sect. 2, taking into account realistic models for the self-interference. First, we analyze the different components that influence the performance. For the performance model, we realistically include protocol overheads, and provide a model for the time spent in overheads, collisions and effective data transmission. A detailed hardware and physical layer model for the full-duplex operation is also considered, affecting the noise but also hardware energy consumption. Subsequently, we end this section with a throughput model, considering the noise and protocol overheads. The energy model is further discussed in the next section.

In the following sections, we focus on Institute of Electrical and Electronics Engineers (IEEE) 802.15.4 nodes as this standard is often used in wireless sensor networks. To reduce modeling complexity, we focus on unacknowledged packets, where packets are always detected except in the presence of collisions, interference or other noise sources. Moreover, the material presented here focuses on uncoded transmissions, which is consistent with the IEEE 802.15.4 standard, while an extension to coded transmissions is possible using the results from [23]. Finally, we consider networks in a star topology with one central node, leaving issues related to routing for future work.

In this section, we look at how decoding errors, collisions and interference affect the link performance, defined by the average time required per successfully transmitted bit. The average time per successfully transmitted bit ($\bar{T}$) reflects the time a wireless device is actively using the wireless spectrum to transmit data, and can be expressed as

$$\bar{T} = T_{\mathrm{b}}\bar{\tau}_{\mathrm{d}} + T_{\mathrm{i}}\bar{\rho}_{\mathrm{i}} + T_{\mathrm{c}}\bar{\rho}_{\mathrm{c}}, \tag{1}$$

where the first term is due to decoding errors, the second due to interference and the final one due to collisions. $\bar{\tau}_{\mathrm{d}} \geq 1$ is the average number of *transmission trials* to decode the frame error-free given that there are no collisions or interference other than self-interference, $\bar{\rho}_{\mathrm{i}} \geq 0$ is the average number of *retransmissions* due to interference given that there are no collisions and $\bar{\rho}_{\mathrm{c}} \geq 0$ is the average number of *retransmissions* due to collisions. T_{b} is the time per transmitted bit as defined by the physical layer, T_{i} is the time per bit lost before the interference is detected and T_{c} is the time per bit before a collision is detected.

Let us now look at the components that make up (1).

3.1 Transmission trials τ_{d} due to decoding errors

T_{b} is mainly dependent on parameters defined by the Physical Layer (PHY). T_{b} consists of the time to transmit the header, T_{H}, the payload, T_{P} and the overhead signals for channel estimation, synchronization, etc., T_{O}. Dividing the sum by the total amount of data bits in the payload, L_{P}, gives the airtime per payload bit

$$T_{\mathrm{b}} = \frac{T_{\mathrm{P}} + T_{\mathrm{H}} + T_{\mathrm{O}}}{L_{\mathrm{P}}}. \tag{2}$$

By denoting the physical layer symbol rate as R_{s} and the number of bits per symbol as b, one can rewrite T_{b} as

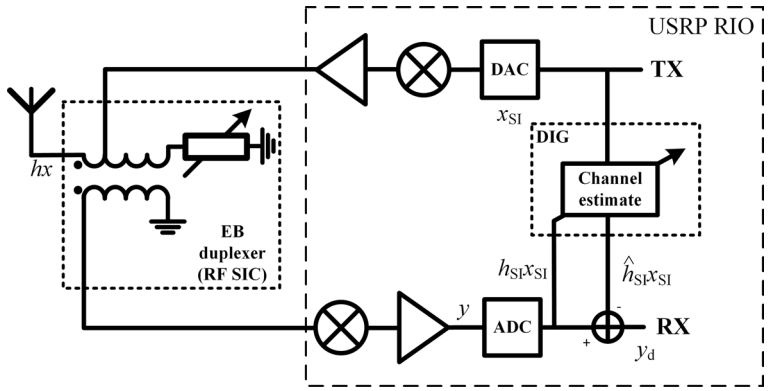


Fig. 4 In-band full-duplex architecture used in the measurements and mathematical modeling

$$T_b = \frac{1}{bR_s}\left(1 + \frac{L_H}{L_P} + \frac{L_O}{L_P}\right), \tag{3}$$

where L_H is the number of bits of header and L_O correspond to the cost of the overhead—measured in bits.

$\bar{\tau}_d$ is also dependent on PHY parameters such as the channel statistics, signal-to-noise ratio (SNR), modulation, code rate and frame size [24]. The SNR is not only dependent on the distance but also on the SIC. We therefore model the remaining self-interference based on measurements from our IBFD prototype using an electrical balance-duplexer [25] and a Universal Software Radio Peripheral (USRP) RIO, as shown in Fig. 4.

In an IBFD system, the received signal after analog cancellation, but before digital cancellation (cf. Fig. 4), can be expressed as

$$y = hx + h_{SI}x_{SI} + w_n, \tag{4}$$

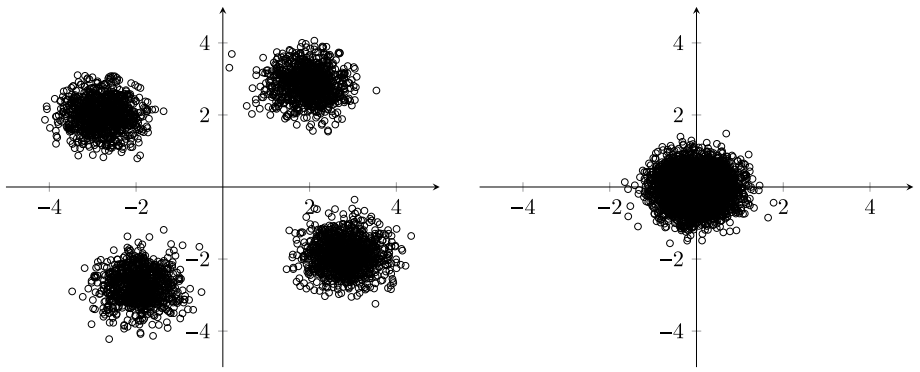
where hx is the useful signal coming from the other node, $h_{SI}x_{SI}$ is the remaining self-interference and w_n is the corresponding additive noise term. In general, the interference and noise on the useful signal x is dominated by the self-interference signal.

After digital cancellation, the received signal can be written as

$$y_d = hx + w'_n, \tag{5}$$

where we assume the interference and noise will no longer be dominated by the self-interference and $w'_n = w_n + (h_{SI} - \hat{h}_{SI})x_{SI}$. With $\hat{h}_{SI}$ the least squares estimate from the digital cancellation. In this section we are interested in finding the properties of w'_n.

To measure the self-interference, the IBFD architecture from [26] is used, as shown in Fig. 4. The setup uses the National Instruments USRP RIO platform [27] for the baseband processing. To cancel the self-interference signal in the analog domain, a custom Electrical Balance Duplexer (EBD) [25] is used. The EBD balances the impedance from the antenna in order to create an inverse copy of the SI signal. This inverse copy destructively interferes with the SI signal, achieving a cancellation of at least 50 dB at Radio Frequency (RF). Next, offline digital cancellation is applied, where a least squares estimate of h_{SI}, i.e. $\hat{h}_{SI}$, is obtained. Finally, the reconstructed signal $\hat{h}_{SI}x_{SI}$ is subtracted from the received signal. The combination of these techniques provides over 90 dB cancellation



a Before digital cancellation ($h_{\mathrm{SI}}x_{\mathrm{SI}} + w_{\mathrm{n}}$) **b** After digital cancellation (w'_{n})

Fig. 5 Constellation graph of the measured signals

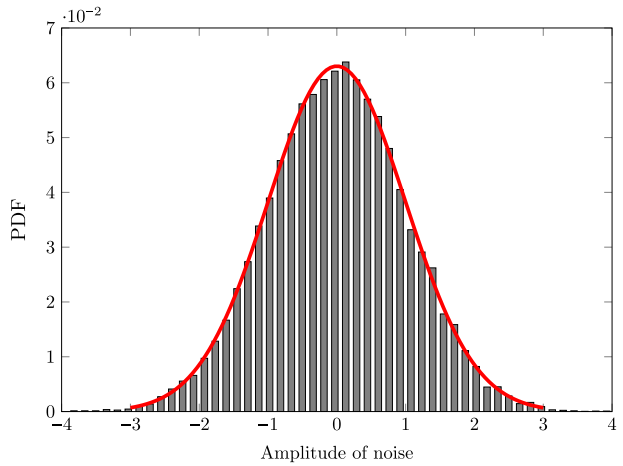


Fig. 6 Histogram of the measured signal after digital cancellation (w'_{n}) with a Gaussian PDF plotted on top

to keep the SNR on a similar level as in the half-duplex case, which is confirmed by our measurements in Figs. 5 and 6.

The USRP transmits a Quadrature Phase Shift Keying (QPSK) modulated signal with a sinc pulse shape. The bandwidth of the signal is 5MHz, consistent with the channel bandwidth of IEEE 802.15.4 [20]. The signal is transmitted through the EBD,, which is configured to give a cancellation of around 50dB. The resulting signal is received again by the second front-end of the USRP. Both the transmitted and received signal as well as the noise w_{n} without any signals present, were logged. Next the signals are loaded into MATLAB, where a custom digital cancellation scheme is ran to estimate h_{SI}.

Figure 5 shows a comparison of the self-interference symbols before digital cancellation ($h_{\mathrm{SI}}x_{\mathrm{SI}} + w_{\mathrm{n}}$) and after digital cancellation (w'_{n}). These figures show that the leakage from the QPSK transmit data is attenuated below the receiver noise floor, and hence prove that the assumptions made in (4) and (5) are valid. From the constellation diagram of Fig. 5b it is not possible to distinguish the self-interference symbols which were still

clearly visible before digital cancellation. However, it is not clear if the noise is dominated by $(h_{\mathrm{SI}} - \hat{h}_{\mathrm{SI}})x_{\mathrm{SI}}$ or w_{n} and what the distribution of the noise is.

To determine this, the distributions of w'_{n} and w_{n} were compared. This can be done using the two-sample Kolmogorov-Smirnov test [28]. Applying this test on both signals shows that both distributions are very similar (asymptotic P-value of more than 0.8), i.e, w'_{n} is dominated by w_{n}. The histogram of the signal after digital cancellation (Fig. 6) clearly follows a Gaussian distribution, demonstrating that the complete SI signal is removed.

Furthermore, most of the evidence found in the literature suggests that h_{SI} follows a Rician distribution[2]. We have validated this assumption using our digital cancellation scheme.

Following the measurement results, it is safe to assume that the noise w'_{n} is Gaussian distributed if analog and digital cancellation are applied. Based on the previous results, we model the Signal-to-Self-Interference-and-Noise Ratio (SSINR) or $\bar{\gamma}$ of a full-duplex link as

$$\bar{\gamma} = \frac{P_{\mathrm{rx}}}{|h_{\mathrm{SI}}|^2 P_{\mathrm{tx}} + P_{\mathrm{n}}}, \tag{6}$$

for the case where only analog cancellation is active. Here P_{rx} is the received signal strength of the useful signal, P_{tx} is the transmitted signal strength of the self-interference signal and P_{n} is the noise power. The self-interference channel, h_{SI} can be considered constant over time during the packet transmission but it is dependent on the frequency. For the case where both analog and digital cancellation are active, we model it as,

$$\bar{\gamma} = \frac{P_{\mathrm{rx}}}{|h_{\mathrm{SI}} - \hat{h}_{\mathrm{SI}}|^2 P_{\mathrm{tx}} + P_{\mathrm{n}}} \approx \frac{P_{\mathrm{rx}}}{P_{\mathrm{n}}} \tag{7}$$

and therefore,

$$\bar{\tau}_{\mathrm{d}}^{\mathrm{HD/CA}} \approx \bar{\tau}_{\mathrm{d}}^{\mathrm{FD/CA}} \approx \bar{\tau}_{\mathrm{d}}^{\mathrm{IB/CD}}. \tag{8}$$

This section proves that even in the case of real self-interference cancellation it is safe to assume that the remaining self-interference after analog and digital cancellation is dominated by Gaussian noise.

In addition, there are collisions and interference that cannot be detected at the transmitter or receiver, as the signal strength from the interfering transmission is too low. This would then increase the noise power P_n for those devices in either half- or full-duplex protocols. These transmissions would normally result in retransmissions due to interference or collisions (i.e. $\bar{\rho}_{\mathrm{i}}$ or $\bar{\rho}_{\mathrm{c}}$), but we assume that packets that cannot be sensed at MAC layer result in PHY problems and are accounted for in $\bar{\tau}_{\mathrm{d}}$ equally for half- and full-duplex protocols. As a result, we assume that the same amount of packets can be detected by each protocol.

[2] For a thoughtful discussion on this issue c.f. [29] and references therein.

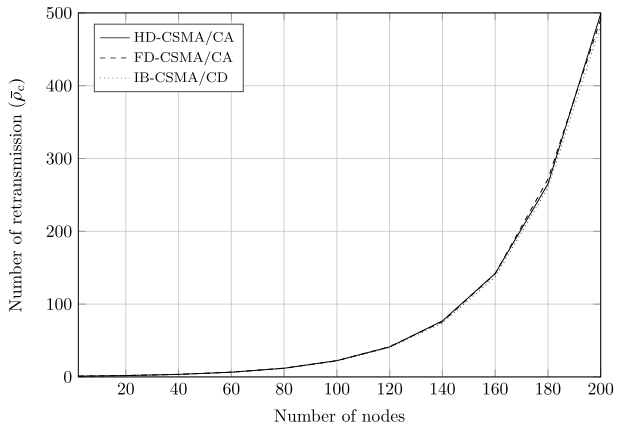


Fig. 7 Validation of the number of retransmission due to collisions in saturated and symmetric traffic conditions

3.2 Retransmissions $\bar{\rho}_i$ due to interference

The total time per payload bit required to detect interference coming from other networks, T_i, can be written also as $T_i = \gamma_i T_b$, where $0 \leq \gamma_i \leq 1$. In the case of HD-CSMA/CA and FD-CSMA/CA, $\gamma_i = 1$ as the interference is only detected at the end of the packet. In the case of IB-CSMA/CD, as interference is usually uncorrelated with the ongoing transmissions, it can occur at any point during the frame, after which it is detected instantaneously. Hence all values $\gamma_i \in (0, 1)$ are equally likely. For the purpose of evaluation, one can consider an average value of $\gamma_i = 1/2$.

It is to be noted that $\bar{\rho}_i$ is independent of the chosen MAC scheme, as it is due to interferers that are uncorrelated with our own transmissions.

3.3 Retransmissions $\bar{\rho}_c$ due to collisions

Following the above rationale, we can rewrite $T_c = \gamma_c T_b$, where for the cases of HD-CSMA/CA and FD-CSMA/CA $\gamma_c = 1$ as there is again no reduction in the time per bit. In the case of IB-CSMA/CD links, collisions can only occur in the beginning of the transmission. This is a consequence of the fact that there are no hidden terminals because of the instantaneous feedback information (c.f. Sect. 2.3). The detection time of a collision is therefore assumed to be equal to the decoding time of the header (assuming it is received with no interference from outside of the considered network). Hence, the time required to detect a packet collision per successfully transmitted bit (goodbit) is

$$T_c = \frac{L_H + L_O}{bR_s L_P}. \tag{9}$$

Note that (9) can be rewritten using (3) as $T_c = \gamma_c T_b$, with

$$\gamma_c = \frac{L_H + L_O}{L_P + L_H + L_O}. \tag{10}$$

This parameter is the fraction of the time per bit, T_b, required to detect a collision. As in general L_P is much larger than L_H and L_O, (10) shows that $\gamma_c \ll 1$.

As this reduction in collision time reduces the congestion of the network, in general, $\bar{\rho}_c^{\mathrm{IB/CD}} \leq \bar{\rho}_c^{\mathrm{FD/CA}}$. Using ns-3, we validated this assumption for saturated traffic conditions (Fig. 7).

3.4 Throughput model

By combining the information from the previous sections we find that the average time per successfully transmitted bit for HD-CSMA/CA is equal to

$$\bar{T}^{\mathrm{HD/CA}} = T_b(\bar{\tau}_d + \bar{\rho}_i + \bar{\rho}_c^{\mathrm{HD/CA}}). \tag{11}$$

For FD-CSMA/CA the average time can be expressed as

$$\bar{T}^{\mathrm{FD/CA}} = \frac{T_b}{2}(\bar{\tau}_d + \bar{\rho}_i + \bar{\rho}_c^{\mathrm{FD/CA}}), \tag{12}$$

if all transmissions occur in full-duplex. And finally the average time per bit for IB-CSMA/CD is equal to

$$\bar{T}^{\mathrm{IB/CD}} = T_b(\bar{\tau}_d + \gamma_i\bar{\rho}_i + \gamma_c\bar{\rho}_c^{\mathrm{IB/CD}}). \tag{13}$$

By neglecting the time lost performing Clear Channel Assessment (CCA) and backoffs, we can define the throughput ($\mathcal{T}$) as the inverse of the average time per bit ($\bar{T}$), i.e.,

$$\mathcal{T} = (T_b\bar{\tau}_d + T_i\bar{\rho}_i + T_c\bar{\rho}_c)^{-1}, \tag{14}$$

therefore lowering the three components on the right hand side increases throughput.

From the previous formulas it is clear that full-duplex transmissions and collision detection will always be better in terms of throughput as the average time per bit is lower, this will be validated in the next section. However, as we will see in Sects. 5 and 6 there is a trade-off in terms of energy efficiency due to the increased power consumption of an IBFD transceiver.

4 Performance results

4.1 Methodology

In this section, we perform ns-3 simulations of IEEE 802.15.4 nodes in a star topology and compute the average number of transmission trials due to collisions, $\bar{\rho}_c$. FD-CSMA/CA and IB-CSMA/CD was implemented on top of the existing IEEE 802.15.4 code of ns-3 version 3.22. In the physical layer, we added extra support for full-duplex communication, while keeping the interface between PHY and MAC identical. In the medium access layer, we added support for our proposed schemes. In any mode, the MAC layer asks the physical layer first to go to RX mode for assessing a CCA. When CCA has successfully ended, the physical layer is asked to go to idle mode and switch to TX mode. Then, after the MAC header is sent or received, full-duplex nodes switch to full-duplex mode. If everything is fine at the receiver side, the receiver answers with either a real-time acknowledgment or a packet for the sender for respectively IB-CSMA/CD or FD-CSMA/CA. If nothing is received, IB-CSMA/CD turns off the transceiver and starts over, while the FD-CSMA/CA scheme switches to half-duplex mode.

Table 1 Parameters used for ns-3 simulations

Parameter	Value
Nodes	2–200
Frame header—L_H	8 bytes[a]
Payload length—L_P	90 bytes[a]
Overhead—L_O	5 bytes[a]
Bit per symbol—b	2[a]
Symbol rate—R_s	125 kS/s [a]

Source: [a] [20]

Each simulation represents one hour, which results in sufficient packet transmissions per node and a relevant average packet error rate defined as the probability that a packet is received by the central node, even for simulations with a high number of nodes. Notice also that the distance between each of the nodes and the central node is exactly the same, i.e., all nodes are placed on a circle. As a result, these nodes have all the same probability of reaching the central node and the node average is the same as the simulation average. Furthermore, each scenario is also simulated 10 times to exclude random artifacts. The reported numbers are the mean performance over all 10 simulations for all nodes.

The set-up of our simulation is as follows: traffic is generated in all nodes as specified below, and all nodes can hear each other perfectly as they are close enough to each other, i.e. no hidden node problems. The rest of the parameters are detailed in Table 1. The parameters are consistent with the IEEE 802.15.4 standard.

Each packet arrival is poison distributed. The three schemes are compared in four throughput scenarios

1 *Saturated, symmetric* both access point and nodes receive a new packet every 5 ms;[3]
2 *Saturated, asymmetric* nodes receive a packet every 5 ms and the access point every 500 ms (i.e. every 100th packet, the access point sends a packet back);
3 *Unsaturated, symmetric* both access point and nodes receive a new packet every 6 s;
4 *Unsaturated, asymmetric* nodes receive a packet every 6 s and the access point every 60 s (i.e. every 10th packet the access point sends a packet back).

4.2 Results and discussion

The throughput, calculated from the number of packets received in ns-3, from the first two scenarios is shown in Fig. 8. Our simulations confirm that in symmetric saturated traffic conditions, FD-CSMA/CA can get double the throughput of HD-CSMA/CA, which is also confirmed in [11]. Figure 8 also shows that the shorter collision time means that the throughput of IB-CSMA/CD is higher than in the HD-CSMA/CA case. In asymmetric saturated traffic conditions, the performance of HD-CSMA/CA and IB-CSMA/

[3] Each transmission, including CCA and Acknowledgment (ACK) is around 5 ms, therefore the nodes will always have at least one packet in their buffer.

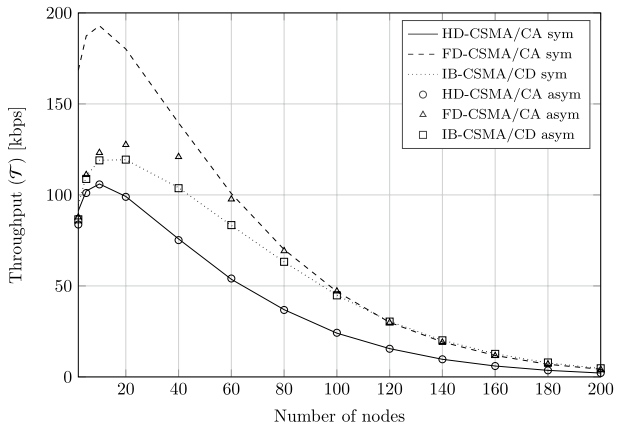


Fig. 8 Saturated scenarios (1 and 2): FD-CSMA/CA increases the throughput in saturated traffic conditions by 2 compared to HD-CSMA/CA. The increase of IB-CSMA/CD compared to HD-CSMA/CA is between 1.2 and 2

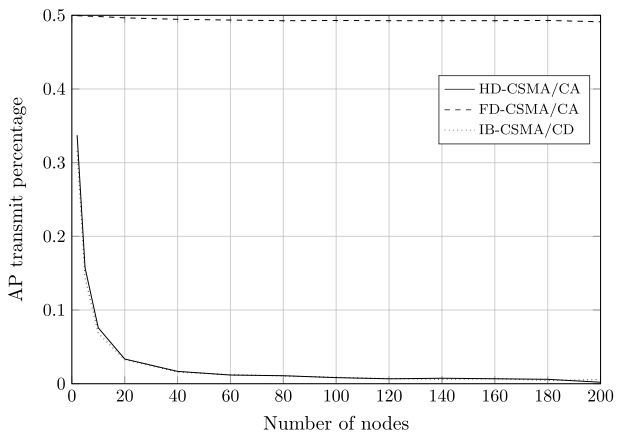


Fig. 9 The AP fairness in symmetric traffic conditions shows that FD-CSMA/CA achieves a fair 0.5 downlink/uplink ratio in all situations while the other two schemes follow a 1/N curve

CD does not change, however, FD-CSMA/CA loses most of its gain due to the fact that most of the transmissions no longer occur in full-duplex.

An important benefit however of FD-CSMA/CA is AP fairness, shown in Fig. 9. In this scheme, the AP always has a slot to transmit data to the nodes, and therefore is able to achieve true symmetric traffic conditions. This is in contrast to the other schemes where the AP has the same amount of transmit opportunities as the other nodes, i.e., $1/N$.

Comparing the throughput for the different protocols in the unsaturated case (Fig. 10), we see that for all three protocols the throughput linearly increases as more and more nodes enter the network. Next, the network starts to get saturated. We find that the throughput benefit of FD-CSMA/CA is not existent.

We can therefore conclude that due to the shorter collision time the throughput of IB-CSMA/CD is higher than HD-CSMA/CA in the saturated scenario and the difference with FD-CSMA/CA is in most cases small. Let us now look at how the three schemes compare in terms of energy consumption.

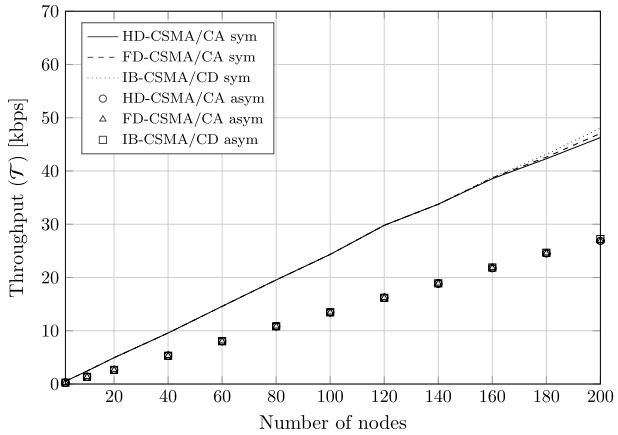


Fig. 10 Unsaturated scenarios (3 and 4): The throughput in unsaturated traffic conditions increases linearly in all schemes. There is no difference in throughput between the different schemes

5 Energy model

In this section we develop a model for the energy consumption of the three types of wireless access studied in Sect. 2.[4] The question we are trying to answer is if the increased energy consumption of an IBFD transceiver can be compensated for by the increased throughput. This model is important as the main cost of the full-duplex technology is in the extra hardware and energy consumption. First, Sect. 5.1 presents the energy modeling of HD-CSMA/CA transmissions, which is then extended in Sects. 5.2 and 5.3 for the cases of FD-CSMA/CA and IB-CSMA/CD links.

5.1 Performance of HD-CSMA/CA

Our goal is to estimate the energy per correctly transmitted data bit, which a node requires for exchanging data with the central node in a network with star topology. In the case of HD-CSMA/CA links, nodes turn on their transmitter or receiver modules sequentially. In half-duplex networks, the total transmit energy consumption per successfully transferred bit can be expressed as

$$\bar{\mathcal{E}}_{\text{tx}}^{\text{HD/CA}} = \frac{\left(P_{\text{el,tx}} + P_{\text{PA}}\right)}{\mathcal{T}} = \left(P_{\text{el,tx}} + P_{\text{PA}}\right) T_{\text{b}} \bar{\tau}^{\text{HD/CA}}. \tag{15}$$

Above, the power consumption of the power amplifier is modeled as P_{PA}, the remaining power to transmit a packet as $P_{\text{el,tx}}$ and T_{b} is the average air time per payload bit. The average number of transmission trials until a frame is decoded without errors, $\bar{\tau}^{\text{HD/CA}}$, can be decomposed as

$$\bar{\tau}^{\text{HD/CA}} = \bar{\tau}_{\text{d}} + \bar{\rho}_{\text{i}} + \bar{\rho}_{\text{c}}^{\text{HD/CA}}. \tag{16}$$

The total energy required by a node to receive one bit of data successfully using HD-CSMA/CA transmissions can then easily be expressed as

[4] This model is an extension of what was presented in [16, 17].

$$\bar{\mathcal{E}}_{\mathrm{rx}}^{\mathrm{HD/CA}} = \frac{P_{\mathrm{el,rx}}}{\mathcal{T}} = P_{\mathrm{el,rx}} T_{\mathrm{b}} \bar{\tau}^{\mathrm{HD/CA}}, \tag{17}$$

where $P_{\mathrm{el,tx}}$ is the electronic consumption of the receiver components.

To consider asymmetric traffic conditions, we introduce the parameter u that represents the percentage of bits transmitted in the uplink, and hence $1-u$ is the percentage of bits received in the downlink. Finally, the average consumption per information bit of a given node is given by

$$\bar{\mathcal{E}}_{\mathrm{b}}^{\mathrm{HD/CA}} = u\bar{\mathcal{E}}_{\mathrm{tx}}^{\mathrm{HD/CA}} + (1-u)\bar{\mathcal{E}}_{\mathrm{rx}}^{\mathrm{HD/CA}} \tag{18}$$

$$= \left[u(P_{\mathrm{el,tx}} + P_{\mathrm{PA}}) + (1-u)P_{\mathrm{el,rx}}\right] T_{\mathrm{b}} \bar{\tau}^{\mathrm{HD/CA}}. \tag{19}$$

5.2 Performance of FD-CSMA/CA

In contrast to HD-CSMA/CA, the nodes using FD-CSMA/CA keep both transmitter and receiver modules active. On top of this, the SIC needs to be active as well. In the sequel, Sect. 5.2.1 analyzes the cost of the SIC module, and Sect. 5.2.2 summarizes our FD-CSMA/CA energy consumption model.

5.2.1 Energy consumption SIC

The SIC module is in general composed by an analog and a digital cancellation submodule, each of which have independent energy requirements. The optimal working point of both SIC components is dependent on impedance variations of the antenna and reflections from the environment. Therefore, we assume that these components need to be retuned every packet transmission. In our proposed architecture, the analog SIC module is composed of an EBD (c.f. Sect. 2). The EBD is a passive component that does not consume power during the frame transmission, only requiring energy during the tuning of the balance network. The energy consumption of the EBD per data bit per transmission trial is given by

$$\mathcal{E}_{\mathrm{EBD}} = \frac{P_{\mu\mathrm{C}} T_{\mathrm{EBD}}}{L_{\mathrm{p}}}, \tag{20}$$

where $P_{\mu\mathrm{C}}$ and T_{EBD} are respectively the power and time consumed by the microprocessor to find an optimal working point for the EBD.

The energy consumption of the digital SIc module per data bit is given by

$$\mathcal{E}_{\mathrm{DIG}} = P_{\mathrm{FIR}} \left(\frac{T_{\mathrm{FIR}}}{L_{\mathrm{p}}} + T_{\mathrm{b}} \right), \tag{21}$$

where P_{FIR} is the power consumption of the Finite Impulse Response (FIR) filter and T_{FIR} is the time it takes to estimate the channel. In contrast with the analog cancellation, digital cancellation consumes power not only while configuring the FIR filter but also during the frame transmission, this introduces an additional term (T_{b}).

Finally, the energy per bit for the full SIC scheme of our architecture is given by

$$\mathcal{E}_{\text{SIC}} = \chi_1 \mathcal{E}_{\text{EBD}} + \chi_2 \mathcal{E}_{\text{DIG}} := P_{\text{SIC}}^{(\text{d})} T_{\text{b}} + \mathcal{E}_{\text{SIC}}^{(\text{s})}, \tag{22}$$

where χ_1 and χ_2 are indicator variables which are equal to 1 if the corresponding module is active and 0 if it's not. Above we are introducing the shorthand notation $P_{\text{SIC}}^{(\text{d})} = \chi_2 P_{\text{FIR}}$ for the power consumption that corresponds to the costs that are proportional to the transmission time T_{b}, and $\mathcal{E}_{\text{SIC}}^{(\text{s})} = (\chi_1 P_{\mu\text{C}} T_{\text{EBD}} + \chi_2 P_{\text{FIR}} T_{\text{FIR}})/L_{\text{p}}$ that is equal to the "static" energy consumption that does not grow with T_{b}.

5.2.2 Total energy consumption

In an IBFD link the receiver module of the transmitter is active during the transmission of data in the uplink to receive downlink data simultaneously. However, some of the electrical components of the transmitter front-end, like the clock generation, can be shared with the receiver front-end, therefore the power consumption of the electronic components is smaller than $P_{\text{el,tx}} + P_{\text{el,rx}}$. We introduce a parameter $0 < \alpha < 1$, such that power consumption of the electronic components of a full-duplex transceiver is equal to,

$$P_{\text{el,FD}} = P_{\text{el,tx}} + \alpha P_{\text{el,rx}}. \tag{23}$$

With this, and following a similar rationale than the one that led to (15), the energy consumption per transmitted goodbit of the FD-CSMA/CA can be modeled as

$$\bar{\mathcal{E}}_{\text{tx}}^{\text{FD/CA}} = \frac{P_{\text{FD}}}{\mathcal{T}} + \mathcal{E}_{\text{SIC}}^{(\text{s})} \bar{\tau}^{\text{FD/CA}} = \left[P_{\text{FD}} T_{\text{b}} + \mathcal{E}_{\text{SIC}}^{(\text{s})} \right] \bar{\tau}^{\text{FD/CA}}, \tag{24}$$

where we are introducing the shorthand notation $P_{\text{FD}} = P_{\text{el,FD}} + P_{\text{PA}} + P_{\text{SIC}}^{(\text{d})}$ and

$$\bar{\tau}^{\text{FD/CA}} = \bar{\tau}_{\text{d}} + \bar{\rho}_{\text{i}} + \bar{\rho}_{\text{c}}^{\text{FD/CA}}. \tag{25}$$

Note that, as mentioned in Sect. 3, the SNR does not change between half- and full-duplex and therefore the terms $\bar{\tau}_{\text{d}}$ and $\bar{\rho}_{\text{i}}$ remain the same as in (16).

During a full-duplex transmission, both transmitter and receiver modules are active, therefore the energy consumption to receive one goodbit is the same as to transmit it, i.e. $\bar{\mathcal{E}}_{\text{rx}}^{\text{FD/CA}} = \bar{\mathcal{E}}_{\text{tx}}^{\text{FD/CA}}$. When only one of the two nodes in the current transmission has data to send, this scheme reduces to the HD-CSMA/CA scheme. Therefore, by introducing ν^{FD} as the percentage of full-duplex transmissions and using ν as the percentage of half-duplex uplink transmissions, the total average energy consumption per transferred bit can be modeled as

$$\begin{aligned} \bar{\mathcal{E}}_{\text{b}}^{\text{FD/CA}} = [\nu^{\text{FD}} \left(P_{\text{FD}} T_{\text{b}}/2 + \mathcal{E}_{\text{SIC}}^{(\text{s})} \right) + \nu (P_{\text{el,tx}} + P_{\text{PA}}) T_{\text{b}} \\ + (1 - \nu - \nu^{\text{FD}}) P_{\text{el,rx}} T_{\text{b}}] \bar{\tau}^{\text{FD/CA}}. \end{aligned} \tag{26}$$

In the first term, T_{b} is divided by 2 because twice the amount of bits can be transmitted in full-duplex. $\mathcal{E}_{\text{SIC}}^{(\text{s})}$, on the other hand, only depends on the actual amount of transmission attempts ($\bar{\tau}^{\text{FD/CA}}$) and as a result, does not get this discount. When $\nu^{\text{FD}} < 1$, the receiver or the transmitter modules are active and the scheme reduces to the half-duplex case, hence the final two terms in (26). Note that $\nu^{\text{FD}} \in [0, 1]$. Typically, $\mathcal{E}_{\text{SIC}}^{(\text{s})}$ is small compared to P_{FD}. As a result, the highest energy efficiency of this scheme is achieved

under bidirectional throughput, leveraging the full-duplex capabilities. This occurs when the two nodes utilize the link continuously sending data to each other, and hence $\nu^{\mathrm{FD}} = 1$. Note also that the percentage of uplink bits $u = \nu^{\mathrm{FD}}/2 + \nu$.

5.3 Performance of IB-CSMA/CD

In the case of IB-CSMA/CD the electronic cost of transmitter, receiver and SIC modules are the same as for FD-CSMA/CA links. However, the energy cost of collisions is reduced as they are detected before the end of the transmission of the full frame, as discussed in Sect. 3.3. Therefore, the energy consumption per transmitted goodbit of the IB-CSMA/CD scheme can be expressed as

$$\bar{\mathcal{E}}_{\mathrm{tx}}^{\mathrm{IB/CD}} = \frac{P_{\mathrm{FD}}}{\mathcal{T}} + \mathcal{E}_{\mathrm{SIC}}^{(\mathrm{s})}\bar{\tau}^{\mathrm{FD/CD}} \tag{27}$$

$$= P_{\mathrm{FD}}T_{\mathrm{b}}\left(\bar{\tau}_{\mathrm{d}} + \gamma_{\mathrm{i}}\bar{\rho}_{\mathrm{i}} + \gamma_{\mathrm{c}}\bar{\rho}_{\mathrm{c}}^{\mathrm{FD/CD}}\right) + \mathcal{E}_{\mathrm{SIC}}^{(\mathrm{s})}\bar{\tau}^{\mathrm{IB/CD}}. \tag{28}$$

Above, $\bar{\rho}_{\mathrm{c}}^{\mathrm{IB/CD}}$ is the average number of retransmission due to collisions in the case of IB-CSMA/CD transmissions and, similarly to (16), $\bar{\tau}^{\mathrm{IB/CD}} = \bar{\tau}_{\mathrm{d}} + \bar{\rho}_{\mathrm{i}} + \bar{\rho}_{\mathrm{c}}^{\mathrm{IB/CD}}$.

Similarly as in the case of FD-CSMA/CA, the cost to transmit and receive data over a IB-CSMA/CD link is the same and hence $\bar{\mathcal{E}}_{\mathrm{rx}}^{\mathrm{IB/CD}} = \bar{\mathcal{E}}_{\mathrm{tx}}^{\mathrm{IB/CD}}$. However, IB-CSMA/CD links share data in a half-duplex time division fashion, as in-band full-duplex is purely used to receive real-time feedback information about collisions and interference while transmitting. Therefore, in contrast to FD-CSMA/CA, IB-CSMA/CD links cannot transmit and receive data at the same time. Accordingly, the total average energy consumption per bit shared over a IB-CSMA/CD link is

$$\bar{\mathcal{E}}_{\mathrm{b}}^{\mathrm{IB/CD}} = u\bar{\mathcal{E}}_{\mathrm{tx}}^{\mathrm{IB/CD}} + (1-u)\bar{\mathcal{E}}_{\mathrm{rx}}^{\mathrm{FD/CD}} \tag{29}$$

$$= P_{\mathrm{FD}}T_{\mathrm{b}}\hat{\tau}^{\mathrm{IB/CD}} + \mathcal{E}_{\mathrm{SIC}}^{(\mathrm{s})}\bar{\tau}^{\mathrm{IB/CD}}, \tag{30}$$

where we have introduced the shorthand notation $\hat{\tau}^{\mathrm{FD}} := \bar{\tau}_{\mathrm{d}} + \gamma_{\mathrm{i}}\bar{\rho}_{\mathrm{i}} + \gamma_{\mathrm{c}}\bar{\rho}_{\mathrm{c}}^{\mathrm{FD}}$ as the "reduced number of retransmissions". Comparing this with (19) and (26), (30) shows that the benefits provided by IB-CSMA/CD in terms of interference management can be suggestively represented as a reduction in the number of retransmissions required to achieve a correctly decoded frame. Finally, (30) also states that $\bar{\mathcal{E}}_{\mathrm{b}}^{\mathrm{IB/CD}}$ is independent of u, showing that the benefits introduced by IB-CSMA/CD are not affected by possible asymmetries in the traffic conditions.

6 Energy results

6.1 Methodology

In this section, we present numerical evaluations that confirm the results presented in previous sections. For these results, we use the same simulations as in Sect. 4 and combine these with the model from the previous section. The extra parameters used for the numerical evaluations are detailed in Table 2. For T_{EBD}, we estimated this value from

Table 2 Parameters used for numerical evaluations

Parameter	Value
Tx electronic power—$P_{el,tx} + P_{PA}$	30.67 mW*
Rx electronic power—$P_{el,rx}$	35.28 mW*
Full-duplex power ratio—α	0.7449$^{\diamond}$
Microprocessor power—$P_{\mu C}$	13.53 mW §
FIR power—P_{FIR}	200 μW ‡
EBD control time—T_{EBD}	128 μs
FIR control time—T_{FIR}	128 μs

From datasheet of *TI CC2420. *Source*: $^{\diamond}$ [15], ‡ [30], § [31]

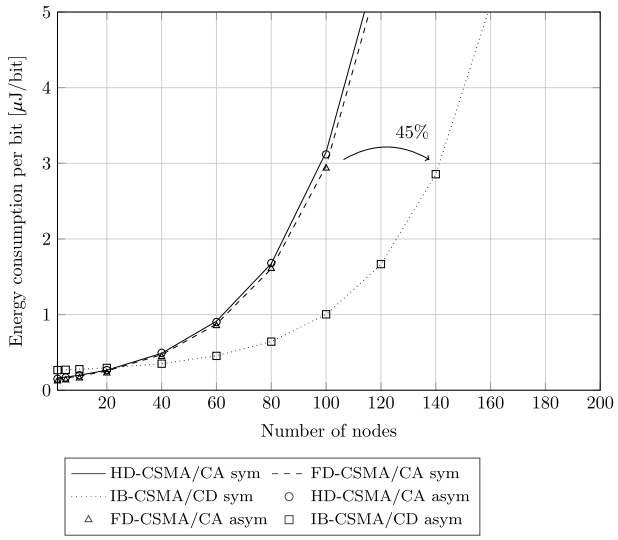


Fig. 11 Saturated scenarios (1&2): The average energy consumption with no interference in saturated traffic conditions shows that IB-CSMA/CD is more energy efficient if more than 20 nodes are in the network compared to HD-CSMA/CA and FD-CSMA/CA

real-world experience with the electrical balance duplexer. The FIR power consumption corresponds to a 4-tap 10 bit filter in 90 nm technology [30].

6.2 Results and discussion

First, in Fig. 11, the energy per bit of the three schemes is compared in saturated symmetric traffic conditions. This condition occurs for example during video conferencing where an equal amount of data is transmitted and received. Symmetric traffic gives the highest energy efficiency to FD-CSMA/CA, as all transmissions can take place in full-duplex. However, our results show that FD-CSMA/CA is only more energy-efficient than IB-CSMA/CD when the number of nodes is low. In effect, Fig. 11 shows that when the network density grows, the performance of IB-CSMA/CD scales more gracefuly, e.g., between 10 and 100 nodes, the energy per bit increases 18-fold for HD-CSMA/CA, while for IB-CSMA/CD this increase happens at 150 nodes. For the same energy consumption, IB-CSMA/CD allows up to 45% more nodes in the network compared to half-duplex and full-duplex transmissions. This is a consequence of the reduced cost of

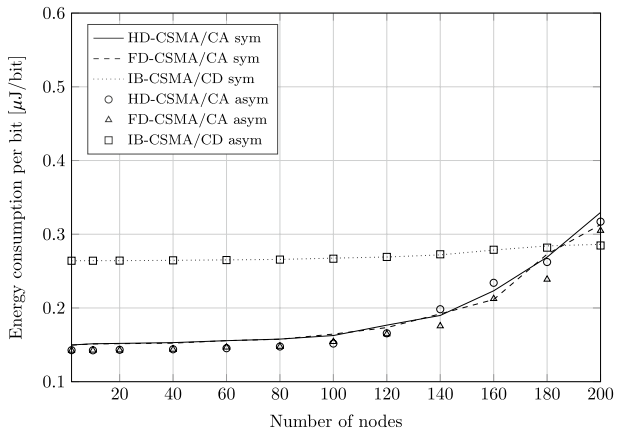


Fig. 12 Unsaturated scenarios (3&4): In unsaturated traffic conditions, the average energy consumption with no interference shows only a minor difference between the three cases

collisions provided by the instantaneous feedback. Comparing HD-CSMA/CA with IB-CSMA/CD, we see a very small difference in average energy per bit. This shows that the increased throughput of Fig. 8 does not outweigh the increased energy consumption of a full-duplex transceiver. When compared in asymmetric traffic conditions, the results do not vary significantly. The only difference is that u^{FD} in (26) becomes small and most transmission happen in half-duplex for FD-CSMA/CA.

Looking at the average energy per bit in unsaturated traffic conditions in Fig. 12, it is clear that for HD-CSMA/CA and FD-CSMA/CA there is again only a small difference as u^{FD} is close to zero because there are not any full-duplex opportunities due to the empty packet buffers. Therefore the scheme is reduced to HD-CSMA/CA. The energy difference between two schemes and IB-CSMA/CD is small however for networks with less than 180 nodes and low traffic, it consumes more power.

Notice that similar findings have been published in [17]. There, the derived equations were evaluated for both IEEE 802.11 and IEEE 80.15.4. For both standards, collision detection was shown to enhance wireless communication. However, the paper also mentioned that several contending devices were required for IEEE 802.15.4, before the protocol could benefit from the extra power consumption of the SIC.

7 Conclusion

In this paper, we analyzed the performance and energy benefits of in-band collision and interference detection. To compare this scheme with half-duplex and symmetric in-band full-duplex transmissions, we developed a communication and energy consumption model, whose key parameters were instantiated using the results of extensive ns-3 simulations.

In terms of throughput, our results suggest FD-CSMA/CA performs better than the other considered schemes under saturated traffic. The advantage is due to the leveraging of the double throughput, which is enabled by the full-duplex communication technology. The throughput gain with respect to IB-CSMA/CD vanishes for networks with 100 or more active nodes, this is because of the shorter collision time of the latter. Also, both schemes always perform better than HD-CSMA/CA. The throughput difference

between collision detection and full-duplex transmissions becomes negligible in unsaturated traffic conditions, where collisions do not hinder the performance significantly.

With respect to energy efficiency, our results show that IB-CSMA/CD outperforms the other two protocols in saturated traffic conditions. For the same energy per bit, this scheme allows 45% more nodes than HD-CSMA/CA. and FD-CSMA/CA to be active in the network. Interestingly, FD-CSMA/CA performs better for a small number of nodes, achieving the highest energy efficiency of the three schemes. Also, the difference between the energy efficiency of the three schemes becomes small in unsaturated traffic conditions.

These results show that in-band collision detection has the capabilities for becoming a key enabling technology for efficient very dense wireless. In effect, the proposed scheme is capable of reducing the energy consumption and increase the number of nodes in the network, while maintaining a high throughput that outperforms half-duplex systems. Therefore, this technology might be an attractive alternative to address crucial networking challenges of wireless networks of the next generation

Abbreviations

ACK: Acknowledgment; AP: Access Point; CCA: Clear Channel Assessment; CSMA: Carrier Sense Multiple Access; CSMA/CA: CSMA Collision Avoidance; CSMA/CD: CSMA Collision Detection; CSMA/CN: CSMA Collision Notification; EBD: Electrical Balance Duplexer; FD-CSMA/CA: Full-Duplex CSMA Collision Avoidance; FIR: Finite Impulse Response; HD-CSMA/CA: Half-Duplex CSMA Collision Avoidance; IB-CSMA/CD: In-Band CSMA Collision Detection; IBFD: In-Band Full-Duplex; IEEE: Institute of Electrical and Electronics Engineers; MAC: Medium Access Control; PHY: Physical Layer; QPSK: Quadrature Phase Shift Keying; RACK: Real-time Acknowledgment; RF: Radio Frequency; SI: Self-Interference; SIC: Self-Interference Cancellation; SNR: Signal-to-Noise Ratio; SSINR: Signal-to-Self-Interference-and-Noise Ratio; USRP: Universal Software Radio Peripheral.

Author's contributions

All authors contributed to the design and evaluation of the schemes and the writing of the manuscript. More specifically, TV implemented the full-duplex physical layer. TV and FER derived and verified the mathematical equations. TV and BR implemented the full-duplex MAC layer in ns-3. SP is the supervisor of TV and BR and guided them in this work. Similarly, MV is the supervisor of FER and guided him during this work. Furthermore, all authors read and approved the final manuscript.

Funding

Tom Vermeulen is funded by the "Agency for Innovation by Science and Technology in Flanders (IWT)". Fernando Rosas was supported by the European Union's H2020 research and innovation programme, under the Marie Skłodowska-Curie Grant Agreement No. 702981. Part of this work is funded under the IWT SBO project SINS and by the KU Leuven OT CAPACITIES under Grant Number OT/14/078.

Availability of data and materials

Will be published on github after acceptance.

Declarations

Competing interests

The authors declare that they have no competing interests.

Author details

[1] ESAT-WAVECORE, KU Leuven, Kasteelpark Arenberg 10, 3001 Heverlee, Belgium. [2] Data Science Institute, Imperial College London, Kensington Campus, London SW7 2AZ, UK. [3] Department of Brain Sciences, Imperial College London, Kensington Campus, London SW7 2DD, UK. [4] Centre for Complexity Science, Imperial College London, Kensington Campus, London SW7 2AZ, UK.

Received: 17 January 2019 Accepted: 9 March 2021
Published online: 08 April 2021

References

1. N. Bhushan, J. Li, D. Malladi, R. Gilmore, D. Brenner, A. Damnjanovic, R. Sukhavasi, C. Patel, S. Geirhofer, Network densification: the dominant theme for wireless evolution into 5g. IEEE Commun. Mag. **52**(2), 82–89 (2014)

2. Deliverable d1.1 deliverable d1.1: scenarios, requirements and KPIs for 5g mobile and wireless system. [Online]. https://www.metis2020.com/wp-content/uploads/deliverables/METIS_D1.1_v1.pdf
3. F. Tobagi, L. Kleinrock, Packet switching in radio channels: part II-the hidden terminal problem in carrier sense multiple-access and the busy-tone solution. IEEE Trans. Commun. **23**(12), 1417–1433 (1975)
4. K. Nishide, H. Kubo, R. Shinkuma, T. Takahashi, Detecting hidden and exposed terminal problems in densely deployed wireless networks. IEEE Trans. Wirel. Commun. **11**(11), 3841–3849 (2012)
5. L. Kleinrock, F. Tobagi, Packet switching in radio channels: part I-carrier sense multiple-access modes and their throughput-delay characteristics. IEEE Trans. Commun. **23**(12), 1400–1416 (1975)
6. E. Ziouva, T. Antonakopoulos, CSMA/CA performance under high traffic conditions: throughput and delay analysis. Comput. Commun. **25**(3), 313–321 (2002)
7. S. Pollin, M. Ergen, S. Ergen, B. Bougard, L. Der Perre, I. Moerman, A. Bahai, P. Varaiya, F. Catthoor, Performance analysis of slotted carrier sense IEEE 802.15. 4 medium access layer. IEEE Trans. Wirel. Commun. **7**(9), 3359–3371 (2008)
8. S. Sen, R.R. Choudhury, S. Nelakuditi, CSMA/CN: carrier sense multiple access with collision notification. IEEE/ACM Trans. Netw. (TON) **20**(2), 544–556 (2012)
9. K. Voulgaris, A. Gkelias, I. Ashraf, M. Dohler, A.H. Aghvami, Throughput analysis of wireless CSMA/CD for a finite user population, in *IEEE Vehicular Technology Conference* (2006), pp. 1–5
10. J. Peng, L. Cheng, B. Sikdar, A wireless MAC protocol with collision detection. IEEE Trans. Mob. Comput. **6**(12), 1357–1369 (2007)
11. Y. Liao, K. Bian, L. Song, Z. Han, Full-duplex MAC protocol design and analysis. IEEE Commun. Lett. **19**(7), 1185–1188 (2015)
12. J.I. Choi, M. Jain, K. Srinivasan, P. Levis, S. Katti, Achieving single channel, full duplex wireless communication, in *Proceedings of the Sixteenth Annual International Conference on Mobile Computing and Networking* (ACM, 2010), pp. 1–12
13. D. Bharadia, E. McMilin, S. Katti, Full duplex radios, in *ACM SIGCOMM Computer Communication Review*, vol. 43, no. 4 (ACM, 2013), pp. 375–386
14. M. Duarte, A. Sabharwal, Full-duplex wireless communications using off-the-shelf radios: feasibility and first results, in *2010 Conference Record of the Forty Fourth Asilomar Conference on Signals, Systems and Computers (ASILOMAR)* (IEEE, 2010), pp. 1558–1562
15. T. Vermeulen, S. Pollin, Energy-delay analysis of full duplex wireless communication for sensor networks, in *2014 IEEE Global Communications Conference (GLOBECOM)* (2014), pp. 455–460
16. T. Vermeulen, F. Rosas, B. van Liempd, M. Verhelst, S. Pollin, An energy-scalable in-band full duplex architecture, in *IEEE Internation Workshop on Computer Aided Modelling and Design of Communication Links and Networks (CAMAD)* (2015)
17. T. Vermeulen, F. Rosas, M. Verhelst, S. Pollin, Performance analysis of in-band full duplex collision and interference detection in dense networks, in *IEEE Consumer Communications and Networking Conference (CCNC)* (2016)
18. G. Bianchi, Performance analysis of the IEEE 802.11 distributed coordination function. IEEE J. Sel. Areas Commun. **18**(3), 535–547 (2000)
19. IEEE Standard for Information technology–Telecommunications and information exchange between systems Local and metropolitan area networks–Specific requirements Part 11, *IEEE 802.11-2012* (2012)
20. IEEE Standard for Local and metropolitan area networks–Part 15.4: Low-Rate Wireless Personal Area Networks (LR-WPANs), *IEEE 802.15.4-2011* (2011)
21. M. Jain, J.I. Choi, T. Kim, D. Bharadia, S. Seth, K. Srinivasan, P. Levis, S. Katti, P. Sinha, Practical, real-time, full duplex wireless, in *Proceedings of the 17th Annual International Conference on Mobile Computing and Networking* (ACM, 2011), pp. 301–312
22. K. Jamieson, H. Balakrishnan, PPR: partial packet recovery for wireless networks, in *ACM SIGCOMM Computer Communication Review*, vol. 37, no. 4 (ACM, 2007), pp. 409–420
23. F. Rosas, R. Souza, M. Pellenz, C. Oberli, G. Brante, M. Verhelst, S. Pollin, Optimizing the code rate of energy-constrained wireless communications with harq. IEEE Trans. Wirel. Commun. **15**(1), 191–205 (2016)
24. F. Rosas, C. Oberli, Modulation and snr optimization for achieving energy-efficient communications over short-range fading channels. IEEE Trans. Wirel. Commun. **11**(12), 4286–4295 (2012)
25. B. van Liempd, B. Hershberg, K. Raczkowski, S. Ariumi, U. Karthaus, K.-F. Bink, J. Craninckx, A +70dbm IIP3 single-ended electrical-balance duplexer in 0.18 um SOI CMOS, in *IEEE International Solid-State Circuits Conference-(ISSCC)* (IEEE, 2015), pp. 32–33
26. T. Vermeulen, B. van Liempd, B. Hershbergt, S. Pollin, Real-time RF self-interference cancellation for in-band full duplex, in *IEEE International Symposium on Dynamic Spectrum Access Networks (DySPAN)* (2015), pp. 275–276
27. NI USRP-2942R-National Instruments [Online]. http://sine.ni.com/nips/cds/view/p/lang/nl/nid/212434
28. F.J. Massey Jr., The Kolmogorov-Smirnov test for goodness of fit. J. Am. Stat. Assoc. **46**(253), 68–78 (1951)
29. M. Duarte, C. Dick, A. Sabharwal, Experiment-driven characterization of full-duplex wireless systems. IEEE Trans. Wirel. Commun. **11**(12), 4296–4307 (2012)
30. K.-S. Kim, K. Lee, Low-power and area-efficient fir filter implementation suitable for multiple taps. IEEE Trans. Very Large Scale Integr. (VLSI) Syst. **11**(1), 150–153 (2003)
31. http://www.atmel.com/Images/Atmel-8266-MCU_Wireless-ATmega128RFA1_Datasheet.pdf

Publisher's Note

Springer Nature remains neutral with regard to jurisdictional claims in published maps and institutional affiliations.